Ahmed Jamal Abdullah AL-Gburi[1], IM Ibrahim[2], M. K. Abdulhameed[3], Z Zakaria[4], M. Y. Zeain[5], Hussam Hamid Keriee[6], Nawres Abbas Nayyef[7], Husam Alwareth[8], Aymen Dheyaa Khaleel[9]

Centre For Telecommunication Research and Innovation (CeTRI), Faculty of Electronic and Computer Engineering, Universiti Teknikal Malaysia Melaka (UTeM), 76100 Durian Tunggal,Melaka
Universiti Teknikal Malaysia Melaka (UTeM), Hang Tuah Jaya, 76100, Durian Tunggal, Melaka, Malaysia
Ministry of Higher Education and Scientific Research, University of Kerbala, Iraq
Communication Engineering Department School of Electrical Engineering Faculty of Engineering Universiti Teknologi Malaysia, Johor

doi:10.15199/48.2021.02.34

A compact UWB FSS single layer with stopband properties for shielding applications

Abstract. *A compact and simple structure of ultra-wideband (UWB) frequency selective surface (FSS) single layer was formed to obtain stopband characteristics in this study. The proposed FSS is made of a modified square loop (MSL) structure with an electrical size of $0.15\lambda_0 \times 0.15\lambda_0 \times 0.041\lambda_0$ and is printed on a single side of the dielectric FR4 substrate. To determine the FSS unit cell structure's behaviour, an equivalent circuit model (ECM) was introduced. Based on the observations, the designed FSS achieved a bandwidth of 10GHz (2.6-12.6 GHz) with -10dB of return loss performance. Hence, the proposed FSS was identified to contribute towards stable angular stability for transverse electric (TE) and transverse magnetic (TM) polarisations from 0° to 45°. Overall, the simulated results were in high-grade harmony compared to the measured results.*

Streszczenie. *Przedstawiono prostą kompaktową antenę szerpokopasmową z możliwością tworzenia pasma zaporowego. Antena ma modyfikowana pętlę kwadratowa o elektrycznym rozmiarze $0.15\lambda_0 \times 0.15\lambda_0 \times 0.041\lambda_0$ I jest drukwana na jednej stronie dielektryka FR4. Na podstawie badań określono pasmo anteny na 2.6 – 12.6 GHz. (**Kompaktowa antena szerokopasmowa z pasmem zaporowym do zastosowań w ekranowaniu**)*

Keywords: MSL-FSS, ECM, TM and TE.
Słowa kluczowe: antena szerokopasmowa, pasmo zaporowe, ekranowanie

Introduction

Frequency selective surface (FSS) is a two-dimensional periodic array exhibiting its filter characteristics to transmit (band-pass) and/or reflect (band-stop) electromagnetic waves (EMW) when triggered by an angle arbitrary to the plane arrays. FSS can be divided into two types: 1) basic element type (such as square loop, square patch, etc.) and 2) fractal type used in many applications (wearable FSS, optical FSS, shielding, absorbers, ultra-wideband (UWB) reflectors, and radomes) [1]–[4].

Primarily, FSS is employed for shielding and UWB antenna performance enhancement applications, particularly for electromagnetic (EM) shielding applications, to prevent the passing of unreliable frequency at specific wavelengths [5], [6]. Moreover, a split-ring resonator (SRR) with stopband behaviour was also used to serve the same purposes [7], [8]. The literature on EM shielding stated that it was developed due to the growing demand for electronic devices with wireless communication technology [9]–[14]. Miniaturised and high-power data rates can be easily influenced nearby other metallic surfaces. Moreover, the radiation from the sources produce electromagnetic interruption (EMI), preventing the device from operating correctly.

FSSs are commonly classified into single and multi-layer configurations. A single FSS layer is designed to deliver an ultrawide stopband filter response for UWB applications [15], [16], In a recent study, Mellita [15] conducted a miniaturised FSS and printed on both sides of a single FR4 dielectric layer. The proposed FSS successfully created a stopband response starting from 1.01 to 9.84 GHz with an FSS unit size of 12×12×1. 6 mm. Another study [16] proposed a single layer of UWB FSS. This proposed FSS was arranged on a sheet of 10 × 10 arrays, whereby the UWB FSS layer was structured and fabricated, covering a bandwidth of 6.9 GHz (4.5-11.4 GHz) with an overall size of 170×170 mm. However, the stopband shielding response did not incorporate the entire UWB characteristics. On the other hand, a multi FSS layer [17] demonstrated that it could exhibit a bandwidth of 7.88 GHz (2.98-10.86 GHz) with -3dB of its return loss performance. Meanwhile, Hua [18] performed a novel UWB FSS with two and a half-dimensional (2.5D) hexagonal ring. The proposed FSS obtained a stopband response from 1.97 to 8.08 GHz with independent transverse agnetic (TM) and transverse electric (TE) polarisation stability. Based on the aforementioned [17], [18] studies, we can conclude that higher resonances are stimulated as the number of layers is increased, resulting in bandwidth improvement of the proposed design. However, the adoption of numerous layers with a large size unit cell in the FSS structure can obstruct the fabrication process and pose financial impacts. Therefore, this study aims to:

1- Achieve a simple structure and small size FSS cell element design as an economical solution, fabricated using the FR4 substrate.
2- Produce a compact FSS single-layer structure to perform a comprehensive stopband response of 2.6 to 12.6 GHz, which covers the UWB (3.1-10.6 GHz), C-band communication satellites (4-8 GHz), and X-band frequency range (8-12 GHz).
3- Achieve a highly angular stability polarisation through TM and TE characteristics.

Hence, this work proposes a compact UWB FSS based on a single-layered structure with wide operating bandwidth. The FSS unit cell geometry is small, with a 5.8×5.8×1.6 mm dimension. While the fractional bandwidth (FBW) of the proposed FSS was approximately 131.6% in introducing a centre-operating frequency (*fc*) at 7.6 GHz. Overall, the FSS single-layer structure is exhibited angular stability through oblique incidence (0° up to 45°).

FSS cell unit design with ECM configuration:

Fig. 1. represents the geometry of the modified square loop (MSL) structure. The metal layer is a combination of an MSL-FSS in periodic array units. The square loop FSS was chosen in this study due to its uncomplicated shape, which makes it perfect for building a prototype for performance assessment. The proportional gaping (*g*) between neighbouring FSS unit cells adopted a capacitance (C) for every unit cell. Fig. 1 also presents the physical dimensions of the length (*Dy*) and the width (*Dx*) of the unit cell.

The ECM configuration describes the operation of this FSS element structure and is displayed in Fig. 2.

In this study, the MSL-FSS structure was first printed on the single side of the FR4 substrate. The horizontal strip (Rs) of the unit obtains an inductance (L1) while the vertical strips (Vs) was increased to obtain an inductance (L2) value.

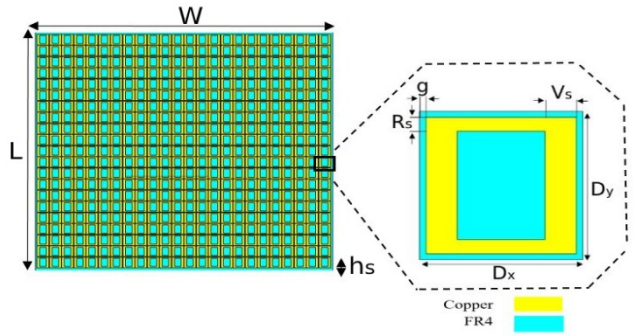

Fig.1. Geometries of the FSSs metallic array and FSS unit cell. where *W*=147, *L*=130, *hs*=1.6, *Dx*= *Dy* =5.8, *Vs*=1.1, *Rs*=0.59 and *g*=0.2. (All dimensions are in mm.

Simultaneously, the gap (g) was reduced to attain a high capacitance (C1) value between the unit cells. Therefore, the stopband response was improved due to the high (C1) between the unit cells. Meanwhile, the empty area inside the MSL structure created a minimal C2, which allows high frequencies to pass through. L1 and C1 are connected in series, while the parallel combination is visible between L2 and C2, as shown in Fig. 2b. The proposed FSS is modelled by equivalent inductance (L) and capacitance (C) lumped components, as shown in Fig. 2a. The proposed circuit model achieves the band-stop behavior at 9.2 GHz, and its impedance is derived in equation (1).
The derived formulation is classified into two zeros and two verticals, as denoted in equation (1).

$$Z_{PFSS} = \frac{\left[\omega^2 C_1 L_2 - (1-\omega^2 C_1 L_1)(1-\omega^2 C_2 L_2)\right]}{j\omega C_1 (1-\omega^2 C_2 L_2)} \quad (1)$$

$$C_2 = \frac{1}{L_2 \omega_{p2}^2} \quad (2)$$

$$C_1 = \frac{(\omega_{p2}^2 - \omega_{z1}^2)(\omega_{p2}^2 - \omega_{z2}^2)}{-L_2 \omega_{p2}^2 \omega_{z1}^2 \omega_{z2}^2} \quad (3)$$

$$L_1 = \frac{\left(\omega_{p2}^2 - \omega_{z1}^2\right) - C_1 L_2 \omega_{p2}^2 \omega_{z1}^2}{C_1 \omega_{z1}^2 (\omega_{p2}^2 - \omega_{z1}^2)} \quad (4)$$

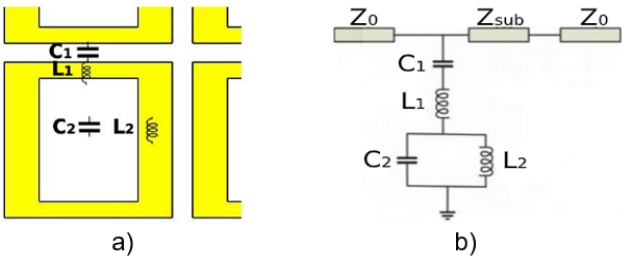

Fig.2. ECM of the proposed MSL. (a) lumped formation (b) ECM.

Table 1. Lumped parameters

ECM values			
C1	C2	L1	L2
0.25pF	0.35pF	0.85nH	0.45nH

In equations (2) to (4), ω_{p2}, ω_{z1}, and ω_{z2} are the vertical and two zeros, sequentially, while the first vertical ωp1 is equal to zero. The binary value of L2 has been embedded continuously to estimate the lumped parameters. It's recorded in Table 1, which is determined by applying the relations mentioned above using advanced design system (ADS) software. The transmission of the proposed MSL-FSS can be approximated by the transmission line theory equation (5) after assessing the lumped parameters as given in [19], [20].

$$S_{21} = \frac{2Z_0}{AZ_0 + B + CZ_0^2 + DZ_0} \quad (5)$$

where variables of A, B, C, and D belong to the matrix of the ABCD, and the number N is the amount of FSS layers.

$$\begin{bmatrix} A & B \\ C & D \end{bmatrix} = [M_{MSLFSS}][M_{n+1}] \dots [M_N] \quad (6)$$

In equation (6), *Mn* is the squandering pattern of the *nth* substrate layer (FR4). In this study, a single substrate layer was used, and the FSS is printed on both sides of the FR4 substrate. Therefore, the formula (6) is determined for a single layer, reducing in formula (7).

$$\begin{bmatrix} A & B \\ C & D \end{bmatrix} = [M_{MSLFSS}][M_1] \quad (7)$$

$$[M_1] = \begin{bmatrix} Cos(k_{z1}d) & jZ_0 \sin(k_{z1}d) \\ j\frac{\sin(k_{z1}d)}{Z_0} & Cos(k_{z1}d) \end{bmatrix} \quad (8)$$

$$[M_{MSLFSS}] = \begin{bmatrix} 1 & 0 \\ 1/Z_{MSLFSS} & 1 \end{bmatrix} \quad (9)$$

A similar method can be modified for determining the TE and TM polarisation, where MSL-FSS in equation (9) is returned with ZTE and ZTM, as provided in the following formulas:

$$Z^{TE} = \frac{\omega \mu_r \mu_0}{k_{z1}} \quad (10)$$

$$Z^{TM} = \frac{k_{z1}}{\omega \varepsilon_r \varepsilon_0} \quad (11)$$

where k_{z1} and k_t are the normal and tangential components of the wavenumber, respectively, and are given in formulas (12) and (13). μr, μ_0 are the relative magnetic permeability in free space. The value of effective permittivity of FR4 substrate (*εeff*) is calculated by *εeff =0.5(εr+1),* where *εr* is the dielectric loss of FR4 substrate equal to 4.4 and θ is the incidence angle, where ε_0 is the relative magnetic permittivity.

$$k_{z1} = \sqrt{\varepsilon_r k_0^2 - k_t^2} \quad (12)$$

$$k_t = k_0 \sin\theta \quad (13)$$

Meanwhile, k_0 denotes the thickness of the FR4 layer.

Simulation and measurement results:

The CST-studio software was implemented for the simulation results to confirm the frequency response received by copying a unit cell. In this study, the proposed FSS layer with 130×147×1.6mm (21×24 unit cells) dimension was developed, tested, and measured. FR4 substrate was used as the dielectric material with a relative dielectric loss of 4.4 and a loss tangent (tan δ) of 0.0009 in this study. The FSS single-layer setup was set within a microwave anechoic chamber and network analyser (NA) with a separation of 1.2 meters connecting the two horn antennas as depicted in Fig. 3. The separation allows an incident plane wave on the FSS layer due to the radiation field condition's satisfaction. The proposed FSS has a UWB stopband response from 2.6 GHz to 12.6 GHz resonating at 9.2 GHz, with a fractional bandwidth (FBW) of 131.6%.
Fig. 4 indicates the angular stability of the simulated and measured transmission coefficient of the proposed FSS for several values (0° up to 45°) of the angle of incidence in TM and TE polarisation. The proposed FSS is explored and examined under TE and TM, respectively.

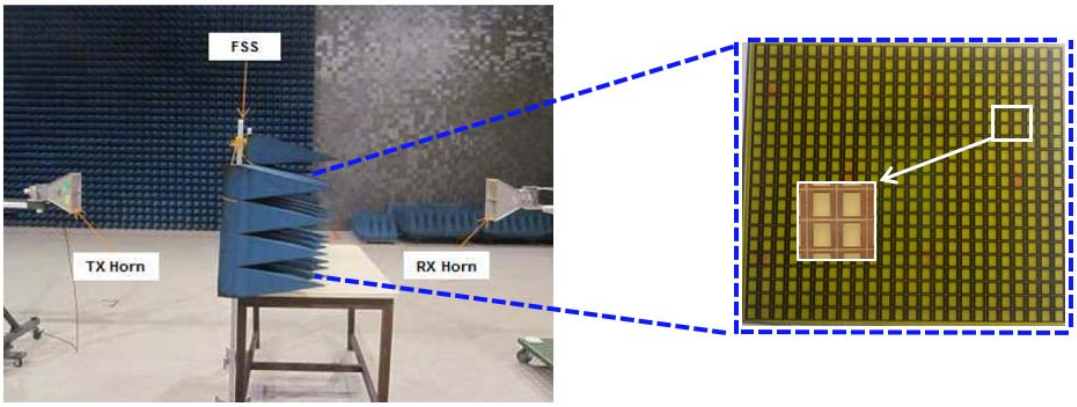

Fig. 3. Measurement setup and fabricated FSS single-layer.

Based on Fig. 4, the proposed FSS provided angular stability across edges up to 45° for TE and TM polarisation starting from a perspective of incidence of 10°

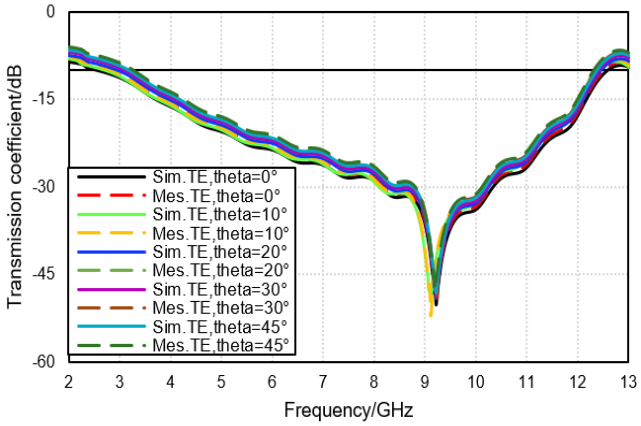

a)

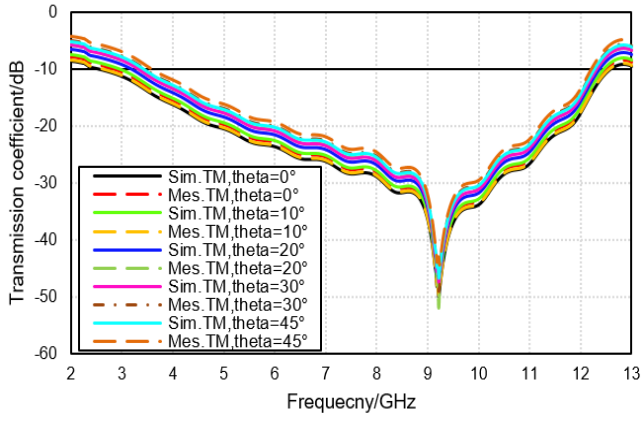

b)

. Fig.4. Transmission Coefficient (S21) of the proposed FSS for different values of the angle of incidence under a) Te-polarisation, b) TM-polarization.

In addition, the modeled FSS is compared with existing FSSs prototypes in Table 2 to differentiate the characteristics. Based on the results, the proposed UWB FSS single-layer structure fulfilled all objectives that were aimed in terms of miniaturisations, ultrawide stopband, angular stability, and economic fabrication.

Table 2. Comparisons with previous literature

Ref	BW range (*fH-fL*) in GHz	Electrical/Physical dimensions of the FSS unit cell	Overall Dimensions in mm	No. of layers
[15]	8.83 (1.01-9.84)	$0.04\lambda_0\times0.04\lambda_0\times0.003\lambda_0$ (12×11.8×1.6 mm)	300×300	1 SL 2 CL
[16]	6.9 (4.5-11.4)	$0.45\ \lambda_0\times0.45\ \lambda_0\times5.3\lambda_0$ (17×17×0.2 mm)	170×170	1 SL 2 CL
[18]	6.11 (1.97-8.08)	$0.19\lambda_0\times0.16\lambda_0\times0.027\lambda_0$ (11.1×9.6×1.6 mm)	307× 310	2 SL 2 CL
TW	10 (2.6-12.6)	$0.15\lambda_0\times0.15\lambda_0\times0.041\lambda_0$ (5.8×5.8×1.6mm)	130×147	1 SL 2 CL

BW=Bandwidth, TW=This Work, SL =Substrate Layer, CL =Conductive Layer.

Conclusion:

A low profile UWB FSS single-layer was proposed in this study. The electrical dimensions of the proposed FSS layer were $3.3\lambda_0\times3.7\lambda_0\times0.04\lambda_0$ while introducing a centre operating frequency at 7. 6 GHz. The overall analysis revealed that the proposed FSS overpowered the limitations of larger size and narrow bandwidth to provide high angular stability and compact unit cells for TE and TM polarisations in oblique incidences (0° up to 45°). The proposed FSS single layer can be useful for many applications such as UWB, C-band communication satellite, and X-band.

***Authors**: Ahmed Jamal Abdullah Al-Gburi, Centre For Telecommunication Research and Innovation (CeTRI), Jalan Hang Tuah Jaya, 76100 Durian Tunggal, Melaka, engahmed_jamall@yahoo.com. Dr. Imran Mohd Ibrahim, Centre for Telecommunication Research and Innovation (CeTRI), Faculty of Electronic and Computer Engineering, Universiti Teknikal Malaysia Melaka (UTeM), Jalan Hang Tuah Jaya, 76100 Durian Tunggal, Melaka, imranibrahim@utem.edu.my. Dr. Muhannad Kaml Abdulhameed, Ministry of Higher Education and Scientific Research, University of Kerbala, Iraq, Karbala 56001, Iraq, eng_mka@yahoo.com . Prof.Dr. Zahriladha Zakaria, Centre For Telecommunication Research and Innovation (CeTRI), Jalan Hang Tuah Jaya, 76100 Durian Tunggal, Melaka, zahriladha@utem.edu.my . Mohammed Yousif Zeain, Centre for Telecommunication Research and Innovation (CeTRI), Jalan Hang Tuah Jaya, 76100 Durian Tunggal, Melaka, eng.moh1010@gmail.com . Hussam Hamid Keriee, Universiti Teknologi Malaysia 81310 Skudai, Johor Bahru, Johor, Malaysia, Sam22.utm@gmail.com . Nawres Abbas Nayyef, , Centre For Telecommunication Research and Innovation (CeTRI), Jalan Hang Tuah Jaya, 76100 Durian Tunggal, Melaka, Nawrasabbas1@gmail.com . Husam Alwareth, Centre For Telecommunication Research and Innovation (CeTRI), Jalan Hang Tuah Jaya, 76100 Durian Tunggal, Melaka, hussam.w@hotmail.com .Dr. Aymen Dheyaa Khaleel, Universiti Kebangsaan Malaysia, 43600 UKM, Bangi Selangor, Malaysia, son_dragon@yahoo.com .*

REFERENCES

[1] A. J. A. Al-gburi, I. M. Ibrahim, M. Y. Zeain, and Z. Zakaria, “Compact Size and High Gain of CPW-fed UWB Strawberry Artistic shaped Printed Monopole Antennas using FSS Single Layer Reflector,” *IEEE Access*, vol. 8, no. 5, pp. 92697–92707, 2020.

[2] M. USMAN, H. ALSAIF, H. ALSAIF, and S. M. ASIF, “Design of Compact Ultra-Wideband Monopole Semi-Circular Patch Antenna for 5G wireless communication networks,” *Przegląd Elektrotechniczny*, vol. 2, no. 4, pp. 223–226, 2019.

[3] A. Y. I. Ashyap, Z. Z. Abidin, S. H. DAHLAN, and H. A. MAJID, “Highly Efficient Wearable CPW Antenna Enabled by EBG-FSS Structure for Medical Body Area Network Applications,” *IEEE Access*, vol. 6, no. 11, pp. 77529–77541, 2018.

[4] A. J. A. Al-Gburi, I. Ibrahim, and Z. Zakaria, “Gain Enhancement for Whole Ultra-Wideband Frequencies of a Microstrip Patch Antenna,” *J. Comput. Theor. Nanosci.*, vol. 17, no. 2–3, pp. 1469–1473, 2020.

[5] R. S. Anwar, L. Mao, and H. Ning, “Frequency Selective Surfaces : A Review,” *Appl. Sci. 2018*, vol. 8, no. 9, p. 1689, 2018.

[6] D. Sood and C. C. Tripathi, “Polarization Insensitive Compact Wide Stop-band Frequency Selective Surface,” *J. Microwaves, Optoelectron. Electromagn. Appl.*, vol. 17, no. 1, pp. 53–64, 2018.

[7] A. J. A. Al-gburi, I. M. Ibrahim, and Z. Zakaria, “Band-notch effect of U-shaped split ring resonator structure at ultra wide-band monopole antenna Band-notch Effect of U-shaped Split Ring Resonator Structure at Ultra Wide-band Monopole Antenna,” *Int. J. Appl. Eng. Res.*, vol. 12, no. 15, pp. 4782–4789, 2017.

[8] I. M. Ibrahim, A. J. A. Al-gburi, Z. Zakaria, and H. A. Bakar, “Parametric Study of Modified U-shaped Split Ring Resonator Structure Dimension at Ultra-Wide-band Monopole Antenna,” *J. Telecommun. Electron. Comput. Eng.*, vol. 10, no. 2–5, pp. 53–57, 2018.

[9] H. H. Keriee, M. K. A. Rahim, N. A. Nayyef, Z. Zakaria, and A. J. A. Al-Gburi, “High gain antenna at 915 MHz for off grid wireless networks,” *Bull. Electr. Eng. Informatics*, vol. 9, no. 6, pp. 2449–2454, 2020.

[10] A. J. A. Al-Gburi, I. Ibrahim, and Z. Zakaria, “A Miniature Raspberry Shaped UWB Monopole Antenna based on Microwave Imaging Scanning Technique for Kidney Stone Early Detection,” *Int. J. Psychosoc. Rehabil.*, vol. 24, no. 2, pp. 1755–1763, 2020.

[11] A. J. Abdullah Al-Gburi, I. M. Ibrahim, Z. Zakaria, and A. D. Khaleel, “Gain Improvement and Bandwidth Extension of Ultra-Wide Band Micro-Strip Patch Antenna Using Electromagnetic Band Gap Slots and Superstrate Techniques,” *J. Comput. Theor. Nanosci.*, vol. 17, no. 2–3, pp. 985–989, 2020.

[12] H. Alsariera *et al.*, “Compact CPW-Fed Broadband Circularly Polarized Monopole Antenna with Inverted L-shaped Strip and Asymmetric Ground Plane,” *Przegląd Elektrotechniczny*, vol. 8, pp. 53–56, 2020.

[13] M. Y. Zeain, Z. Zakaria, M. Abu, and A. J. A. Al-Gburi, “Design of Helical Antenna for Next Generation Wireless Communication,” *Przegląd Elektrotechniczny*, vol. 11, pp. 96–99, 2020.

[14] M. Y. Zeain, M. Abu, A. J. A. Al-gburi, Z. Zakaria, R. Syahputri, and A. Toding, “Design of a wideband strip helical antenna for 5G applications,” *Bull. Electr. Eng. Informatics*, vol. 9, no. 5, pp. 1958–1963, 2020.

[15] R. A. Mellita, D. S. Chandu, S. S. Karthikeyan, and P. Damodharan, “A Miniaturized Wideband Frequency Selective Surface with Interconnected Cell Structure,” *AEU - Int. J. Electron. Commun.*, vol. 120, no. 4, p. 153196, 2020.

[16] H. J. Kim, S. S. Cho, O. B. Kwon, Y. J. Kim, and I. P. Hong, “Paper-based uniplanar ultra-wideband frequency-selective surface design,” *Electron. Lett.*, vol. 55, no. 9, pp. 506–508, 2019.

[17] S. Unaldi, N. B. Tesneli, and S. Cimen, “A novel miniaturised polarisation independent frequency selective surface with UWB response,” *Radioengineering*, vol. 27, no. 4, pp. 1012–1017, 2018.

[18] B. Hua, X. He, and Y. Yang, “Polarisation-independent UWB frequency selective surface based on 2 . 5D miniaturised hexagonal ring,” *Electron. Lett.*, vol. 53, no. 23, pp. 1502–1504, 2017.

[19] F. Costa, A. Monorchio, and G. Manara, “An Overview of Equivalent Circuit Modeling Techniques of Frequency Selective Surfaces and Metasurfaces,” *Appl. Comput. Electromagn. Soc. J.*, vol. 29, no. 12, pp. 960–976, 2014.

[20] D. Ferreira, S. Member, and R. F. S. Caldeirinha, “Square Loop and Slot Frequency Selective Surfaces Study for Equivalent Circuit Model Optimization,” *IEEE Trans. Antennas Propag.*, vol. 63, no. 9, pp. 3947–3955, 2015.